Electronic Supplementary Material (ESI) for Journal of Materials Chemistry B.

Supplementary data

Investigation of biodistribution and tissue penetration of PEGylated gold nanostars and its application for photothermal cancer treatment in tumor-bearing mice

Chao-Cheng Chen[a,‡], Deng-Yuan Chang[a,‡], Jia-Je Li[a], Hui-Wen Chan[a], Jenn-Tzong Chen[b], Chih-Hsien Chang[b] , Ren-Shyan Liu[a,c,d,e], C. Allen Chang[a,f,g], Chuan-Lin Chen[a,*], and Hsin-Ell Wang[a,*]

[a] National Yang-Ming University, Department of Biomedical Imaging and Radiological Sciences, Taipei, TW.

[b] Institute of Nuclear Energy Research, Taoyuan County, TW.

[c] National Yang-Ming University, Institute of Clinical Medicine Taipei, TW.

[d] National Comprehensive Mouse Phenotyping and Drug Testing Center, Molecular and Genetic Imaging Core/Taiwan Mouse Clinic, Taipei, TW.

[e] Cheng Hsin General Hospital, Department of Nuclear Medicine, Taipei, TW.

[f] National Yang-Ming University, Department of Biotechnology and Laboratory Science in Medicine, Taipei, TW.

[g] National Yang-Ming University, Molecular Imaging Research Center (MIRC), Taipei, TW

* Corresponding author, clchen2@ym.edu.tw (Chuan-Lin Chen); hewang@ym.edu.tw (Hsin-Ell Wang)

‡ These authors contributed equally to this work and should be considered as co-first authors.

Calculation of photothermal conversion efficiency

Two milliliters of pAuNS solution at a concentration of 20 ppm was irradiated with 793 nm laser for 900 s to reach the maximum steady temperature and then cooled down without laser irradiation. The temperature was recorded by a thermal meter every 10 s during this study. We calculated the photothermal conversion efficiency (η) by the following equation[1]:

$$\eta = \frac{hs(T_{Max} - T_{surr}) - Q_{Dis}}{I(1 - 10^{-A_{793}})} \qquad (1)$$

Where *h* is the heat transfer coefficient, *s* is the surface area of the container, and the value of *hS* is obtained from Eq. 4. T_{Max} and T_{surr} represented the maximum steady temperature of the pAuNS solution after 790 nm laser irradiation and the environment temperature, respectively. In this study, T_{Max} of the pAuNS solution and T_{surr} were 49.2 and 24.2°C, respectively. Hence, the temperature change (T_{Max}-T_{surr}) of the pAuNS solution after laser irradiation was 25°C. Q_{Dis} is heat dissipation from the absorbed light by cuvette and pure water, and the value of Q_{Dis} was 51.98 mW. The laser power (*I*) and the absorbance of pAuNS at 793 nm were 1.0 W and 0.92, respectively.

In order to gain the value of *hs*, the dimensionless parameter θ was firstly calculated by the following equation:

$$\theta = \frac{T - T_{surr}}{T_{Max} - T_{surr}} \qquad (2)$$

where *T* is the temperature in the cooling period according to Fig. 4B.

According to Fig. 4B, the sample system time constant (τ_s) can be computed as

$$t = -\tau_s \ln(\theta) \qquad (3)$$

The value of τ_s was 441.92 (s), and it can be used for the following equation for calculating the value of *hS.*

$$hs = \frac{\sum_i m_i \times C_{p,i}}{\tau_s} \qquad (4)$$

where *m* is the mass and *C* is the heat capacity of each *i* component of the sample cell. In this study, the mass of pAuNS solution and quartz cuvette was 2 and 6.07 g, respectively. The heat capacity of pAuNS solution and quartz cuvette was 4.18 and 0.839 J/g·°C, respectively. Hence, the *hs* was calculated to be 0.0304 W/°C. Substituting each parameter in Eq.1, the photothermal conversion efficiency of pAuNS solution (O.D. = 1.0) at a 793 nm laser irradiation was 80.5%.

Calculation of heat flux per mass and heat capacity of pAuNSs

The heat flux per mass and heat capacity of pAuNS at a concentration of 20 ppm was performed based on the previous study.[2]

$$D = \frac{hs(T_{Max} - T_{surr}) - Q_{Dis}}{mass\ of\ solvent\ or\ materials} \qquad (5)$$

Therefore, D_{water} and D_{pAuNS} were 0.355 and 1.77×10^4 W/g.

Assuming no heat loss in this system during this experiment, the temperature increase speed can be calculated by the following equation:

$$Temperature\ increase\ speed = \frac{D}{heat\ capacity\ of\ solvent\ or\ materials} \qquad (6)$$

Hence, the temperature increase speed of water and pAuNS were 0.085 and 1.37×10^5 °C/s.

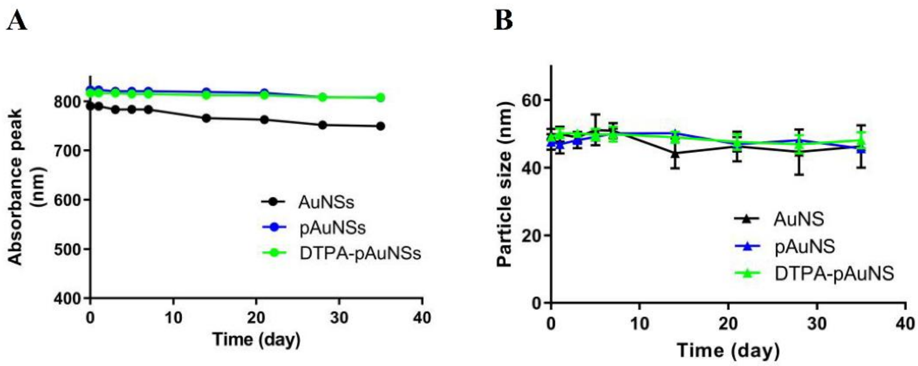

Fig. S1 Physical stability of AuNSs, pAuNSs and DTPA-pAuNSs incubated in deionized water at 4°C. The change of the absorbance peak (A) and particle size distribution (B) were examined using UV-Visible Spectrophotometer and dynamic light scattering, respectively.

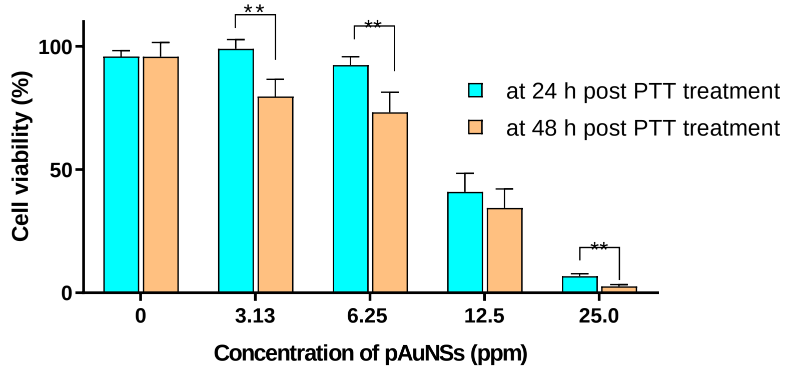

Fig. S2 Relative cell viability of SKOV-3 cells at 24 h or 48 h post PTT treatment. The cell viability was determined by MTT assay. ** indicates $p < 0.01$.

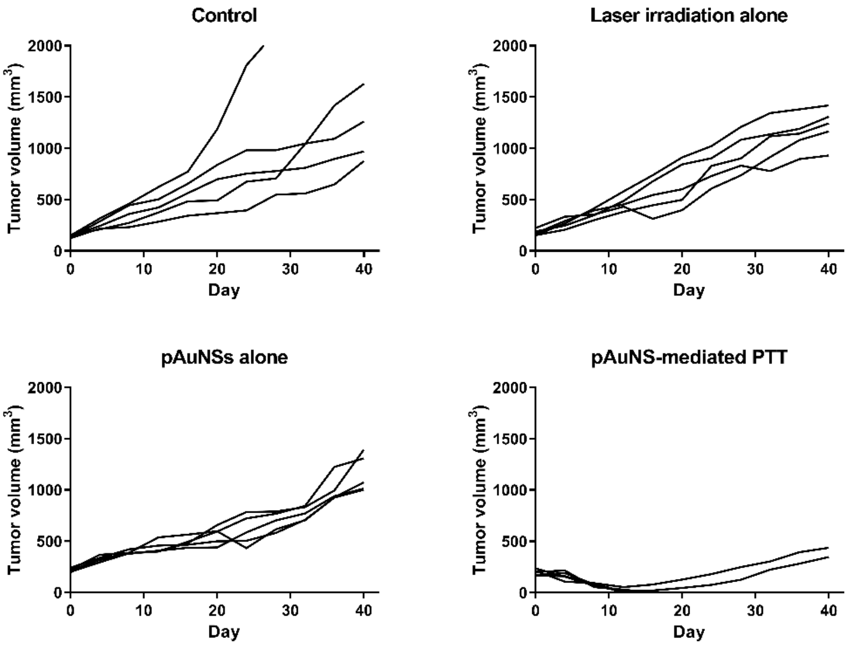

Fig. S3. The tumor burden of each SKOV-3 tumor-bearing mouse in the control, laser irradiation alone, pAuNSs alone and pAuNS-mediated PTT groups.

Table S1. Summary of UV-Vis peak, hydrodynamic diameter, polydispersity index (PDI) and zeta potential of gold nanostars

Gold nanoparticles	Absorption peak (nm)	Hydrodynamic diameter (nm)[1]	PDI	Zeta potential (mV)
AuNSs	791 ± 2.1	46.8 ± 3.6	0.350	-37.41 ± 0.24
pAuNSs	823 ± 3.2	50.5 ± 2.1	0.223	-8.69 ± 2.06
DTPA-pAuNSs	817 ± 3.5	51.4 ± 2.5	0.202	-15.76 ± 1.45

[1], determined by dynamic light scattering; AuNSs, gold nanostars; pAuNSs, PEGylated gold nanostars; DTPA-pAuNSs, DTPA-conjugated PEGylater gold nanostars

Table S2. Photothermal conversion efficiency (η) of gold nanoparticles developed in this study and those reported in literatures.

Photothermal agents	Particle size (nm)	Wavelength of laser (nm)	η	Reference
Gold nanoshells	~40[a]	815	59 %	3
	60	980	61 %	2
	120[c]	808	41.6 %	4
	~180[b]	815	30 %	3
Gold nanorods	7/26 (wide/length)	808	50 %	5
	10/38.9	815	55 %	3
	13/45	808	23.1 %	6
	17/56.1	808	22.1 %	7
Gold nanocages	45	808	63.6 %	7
Gold nanostars	30	980	94 %	2
	50.5	793	80.5 %	This study
	~60[d]	980	78.8 %	8
	60	980	90 %	2
Hexapods	25	808	29.6 %	7
Pathy gold-on carbon nanospheres	185	808	31.6 %	6

a, Au_2S/Au nanoshells; b, SiO_2/Au nanoshells; c, Ag/Au nanoshell; d, spiky Au_6 nanoparticles

Reference

1. C. Ayala-Orozco, C. Urban, M. W. Knight, A. S. Urban, O. Neumann, S. W. Bishnoi, S. Mukherjee, A. M. Goodman, H. Charron, T. Mitchell, M. Shea, R. Roy, S. Nanda, R. Schiff, N. J. Halas and A. Joshi, *ACS nano*, 2014, **8**, 6372-6381.
2. Y. Liu, J. R. Ashton, E. J. Moding, H. Yuan, J. K. Register, A. M. Fales, J. Choi, M. J. Whitley, X. Zhao, Y. Qi, Y. Ma, G. Vaidyanathan, M. R. Zalutsky, D. G. Kirsch, C. T. Badea and T. Vo-Dinh, *Theranostics*, 2015, **5**, 946-960.
3. J. R. Cole, N. A. Mirin, M. W. Knight, G. P. Goodrich and N. J. Halas, *The Journal of Physical Chemistry C*, 2009, **113**, 12090-12094.
4. R. Zhu, Y. Li, X. Zhang, K. Bian, M. Yang, C. Cong, X. Cheng, S. Zhao, X. Li and D. Gao, *Nanotechnology*, 2019, **30**, 055602.
5. V. P. Pattani and J. W. Tunnell, *Lasers in surgery and medicine*, 2012, **44**, 675-684.
6. X. Wang, D. Cao, X. Tang, J. Yang, D. Jiang, M. Liu, N. He and Z. Wang, *ACS applied materials & interfaces*, 2016, **8**, 19321-19332.
7. J. Zeng, D. Goldfeld and Y. Xia, *Angewandte Chemie*, 2013, **52**, 4169-4173.
8. C. Bi, J. Chen, Y. Chen, Y. Song, A. Li, S. Li, Z. Mao, C. Gao, D. Wang, H. Möhwald and H. Xia, *Chemistry of Materials*, 2018, **30**, 2709-2718.